Reconstructing the impact of nickel mining activities on sediment supply to the rivers and the lagoon of South Pacific Islands: lessons learnt from the Thio early mining site (New Caledonia)

Virginie Sellier, Oldrich Navratil, J. Patrick Laceby, Michel Allenbach, Irène Lefèvre, Olivier Evrard

Reconstructing the impact of nickel mining activities on sediment supply to the rivers and the lagoon of South Pacific Islands: lessons learnt from the Thio early mining site (New Caledonia)

Virginie Sellier[1] • Oldrich Navratil[2] • J. Patrick Laceby[3] • Michel Allenbach[4] • Irène Lefèvre[1] • Olivier Evrard[1]

[1]Laboratoire des Sciences du Climat et de l'Environnement (LSCE), UMR 8212 (CEA/CNRS/UVSQ-IPSL), Université Paris-Saclay, Gif-sur-Yvette (France)

[2] Laboratoire Environnement Ville Société (EVS), Université Lumière Lyon 2, UMR 5600 (CNRS), Lyon (France)

[3] Environment and Parks, Calgary, Alberta (Canada)

[4] LIVE-EA 4243, Université de Nouvelle-Calédonie & LABEX Corail, Nouméa (Nouvelle-Calédonie, France)

Corresponding author: selliervirg@free.fr ; Tel: (33)673910072

Abstract

Opencast mining has exacerbated land degradation in New Caledonia, a French archipelago located in the south-west Pacific Ocean. Developed since the 1880s, mining has become the major economic activity in some catchments, which strongly disrupted sediment dynamics. Reconstructing the temporal changes of sediment source contributions is essential to understand the driving factors of soil erosion in response to i) the occurrence of cyclones, ii) the changes in mining practices during the last several decades, and iii) other soil degradation processes such as extensive soil erosion induced by fires, overgrazing and trampling of invasive species, and landslides. Accordingly, a multi-parameter analysis including gamma spectrometry, color and X-ray fluorescence measurements was conducted on a sediment core collected in a deltaic floodplain at the outlet of one of the first areas exploited for nickel mining, the Thio River catchment (397-km²). One geochemical tracer (*i.e.* K) has been used to quantify changes in sediment sources in the successive sediment layers deposited since the beginning of mining activity. The results showed that the contribution of mining tributaries largely dominated, with a mean contribution of 74 % (SD 13 %) of material sampled in the sediment core. This contribution notably increased after the mechanization of mining activities (*i.e.* from 1950s; increase of 18 %). The occurrence of Cyclone Alison in 1975 triggered the progressive transfer of mining waste accumulated on the foothills over 25 years into the river system. This tipping point could be identified in the sediment sequence, which demonstrates that over the last 41 years (*i.e.* 1975-2016), a ~84-cm deep sediment deposit has accumulated in the alluvial floodplain of the Thio River catchment (mean annual deposition rate of 2 cm yr^{-1}). Currently, the progressive release and downstream transfer of this mining waste is still ongoing ~45 years after Cyclone Alison. Although environmental legislation was introduced in 1975, mining tributary contributions to sediment still dominate (80 %, SD 5 %). Overall, this multi-proxy approach to examining the cumulative effects of mining activities on downstream sediment dynamics could be implemented in other mining catchments of New Caledonia and around the world to compare the respective mining source contributions to sediment and their evolution throughout time in these contrasted areas.

Keywords: Soil erosion • sediment fingerprinting • nickel mining • mechanization period

1. Introduction

The ongoing globalization and the growing demand from the increasing world population for food, raw materials and services are causing ever-increasing pressures on the environment. Soil erosion, one of the major global environmental threats, has accelerated in particular in recent decades as a result of changes in landscapes induced by human activities: vegetation clearing and deforestation (Restrepo et al., 2015), crop cultivation (Schmidt et al., 2018), over-grazing, industrialization (Stinchcomb et al., 2013) and urbanization (Russell et al., 2017). Non-renewable soil resources are being depleted (Amundson et al., 2015; Borrelli et al., 2017) while river and coastal systems are being degraded by the excess supply of fine sediment (Syvitski et al., 2005). These impacts are particularly exacerbated in tropical regions exposed to heavy rainfall (Lal, 1983; Restrepo and Syvitski, 2006; Zhu et al., 2008). Tropical depression and cyclone-induced-overbank floods are responsible for most of the sediment transfers observed annually in these river systems (Baltzer and Trescases, 1971; Danloux and Laganier, 1991; Terry et al., 2008). An understanding of the sources, transfer and storage of fine sediment in these river systems is required to guide the implementation of effective management measures. However, the scientific diagnosis of human-induced soil erosion is a challenging problem (García-Ruiz et al., 2017; Muchena et al., 2005). Disentangling the impacts of anthropogenic activities on soil erosion from climatic factors is challenging (Walling and Webb 1996; Restrepo and Syvitski 2006; Raclot et al. 2016). A second factor that may complicate the diagnosis is that multiple anthropogenic activities generally occur during the same timeframe and on the same landscape. Accordingly, it is generally difficult to clearly identify the main human activity controlling soil erosion in a given catchment (Collins and Walling, 2004). Finally, the chronology of anthropogenic activities at the decadal or century scale needs to be considered in order to fully interpret the variability of the current suspended sediment loads in river systems (Dearing et al., 2006; Hoffmann et al., 2010). Suspended sediment fluxes monitored at the outlet can be attributed to current human activities. However, they can also be attributed to the erosion and/or remobilization of legacy sediment mobilized by past human activities, for example agro-pastoralism

(Bajard et al., 2017) or mining activities (Balamurugan, 1991; Coulthard and Macklin, 2003; Navarro et al., 2008).

All these complexities and questions can be found especially in New Caledonia. Indeed, this archipelago, located in the south-west Pacific Ocean holds 25 % of the world nickel resources, making it the sixth largest nickel producer. Started in 1880, mining activities have continued to intensify, particularly with the mechanization of extractive industries from 1950s. This rapid increase of nickel ore production was accompanied by a sharp increase in bare soil areas (*i.e.* mining sites, mining prospection areas and mining roads) and mining waste (Iltis, 1992). In the absence of environmental legislation, 200 million tons of mining waste have been stored on the foothills exposed to rainfall. During the 1970s-1980s, a series of cyclones (*i.e.* Cyclone Colleen in 1969, Cyclone Gyan in 1981 and Cyclone Anne in 1988) hit the archipelago leading to the dumping of this mining waste into the river systems. Since then, the archipelago is confronted with an unprecedented problem of sediment pollution of these river networks: hyper-sedimentation threatening both the inhabitants (*e.g.* increased flooding risk, water pollution by sediment-bound heavy metals) and the island's ecosystems (*e.g.* degradation of coral reef systems). The mining sector, although having contributed largely to New Caledonia's economic growth, is considered to be the main driver of environmental degradation (Bird et al., 1984; Iltis, 1992). This awareness of the environmental impacts of mining activities led to the implementation of the first environmental regulations as early as in 1975 (*e.g.* prohibition of direct dumping of mining waste rocks on the hillslopes) and the adoption of a Mining Code in 2009 (*e.g.* implementation of mitigation hydraulic infrastructures such as retention ponds) aimed at reducing sediment supply to the river network. However, other sources of sediment independent of mining activities may also supply a significant quantity of sediment to New Caledonian river systems and they should be distinguished from mining-related inputs. For instance, bushfires and land clearing fires are regularly triggered by the local population to increase the area of cultivable land (Dumas, 2010). These fires can lead to shallow landslides and/or extensive soil erosion of surface material on hillslopes (Blake et al., 2009; Nyman et al., 2011; Smith et al., 2011). Moreover,

96 the deer population, an invasive species introduced in the early 20th century in New Caledonia,
97 significantly increased during the last 40 years. The associated trampling may have further
98 accelerated surface soil degradation (Shellberg et al., 2010).

99 A recent pilot sediment tracing study was conducted in the Thio River (397 km²) catchment
100 draining the archipelago's first mine (Sellier et al., 2020) to estimate the contributions of sediment
101 sources during two recent cyclonic events (*i.e.* Cyclone Marcia in 2015 and Cyclone Cook in 2017).
102 The authors showed that the spatial distribution of rainfall generated by these two events may
103 locally modify the respective contributions of non-mining and mining tributaries. However,
104 tributaries draining mining sources dominated the sediment supply to the main stem of the Thio
105 River during these two events: 68 % (SD 28 %) in 2015 and 86 % (SD 7 %) in 2017. However, several
106 research questions remained after this first investigation: Do the recently observed mining
107 contributions correspond to the past and/or current mining source contributions? Are these
108 contributions from mining sources significantly lower than those potentially observed at the time of
109 the intensification of mining activities (i.e. from 1950s)? In other words, did environmental
110 regulations lead to a reduction of sediment inputs? To answer these questions, the temporal changes
111 of sediment source contributions should be reconstructed since the beginning of mining activities.
112 Indeed, reconstructing these contributions is essential to understand the driving factors of soil
113 erosion in early mining catchments of the South Pacific Islands in response to i) the occurrence of
114 cyclones, ii) the changes in mining practices during the last several decades, and iii) the occurrence of
115 other soil erosion processes. This ultimate goal of our research is to understand the environmental
116 impacts of the current mining activities into a broader historical context of sediment erosion, and
117 thus to better understand the sediment legacy of the past mining activities. In a post-colonial context
118 of empowerment, this country cannot make its economy sustainable without extractive industries
119 that represent ~5 % of the GDP and ~88 % of the exports in 2016; it has therefore to face challenges
120 related to their development, although it is associated with major socio-environmental concerns:
121 public health, conciliation with other economic activities (*e.g.* agriculture, fishery and tourism),

respect of cultural rights of local communities (Horowitz et al., 2018), and the preservation of biodiversity (Fernandez et al., 2006). This knowledge is therefore essential to inform the choices of a development policy for the mining sector and its management in New Caledonia for the coming decades.

To this end, a multi-parameter analysis based on gamma spectrometry, color and X-ray fluorescence measurements was conducted to a sediment core collected in the alluvial plain of the Thio River catchment. This sediment core recorded the overbank floods and the intensive soil erosion events that occurred over the last several decades. The objective of the current research is to i) identify the flood deposits in this sediment core, ii) estimate by sediment fingerprinting methods the sediment source contribution, iii) provide a dating of the sediment core in order to (iv) discuss the evolution of these contributions in relation to the history of the Thio River catchment and its mining activity.

2. Materials and methods

2.1. Study area

Located on the eastern coast of the New Caledonian archipelago's main island, called *la Grande Terre* (*ca*. 17 000 km²), the Thio River catchment (397 km²) has been mined for nickel since the 1880s. This catchment, like the rest of the archipelago, owes its abundance of minable nickel ores to the widespread occurrence of peridotite massifs (*e.g.* harzburgite, dunite). Indeed, the weathering of the peridotite results in the formation of Ni- and Fe-rich smectite, serpentine, goethite and hematite. The migration of these transition metals through the soil profile results in higher Ni concentrations in the saprolite (Ni: 0.5-3.5 %) and laterite layers (Ni: 0.9-1.8 %) (Trescases, 1973). Peridotite massifs composed of laterites (18 % of the Thio River catchment area), peridotites (17 %), serpentines (10 %) and hazburgites (1 %) are mainly located on the eastern part of this catchment (Garcin et al., 2017) (Figure 1- a). The mountainous relief of the peridotite massifs (*i.e.* with a mean

altitude of 477 m asl, above sea level) contrast with the flatter western part of the catchment of volcano-sedimentary formation rocks (*i.e* with a mean altitude of 368 m asl). These rocks are composed of cherts (22 %), sandstone (9 %), a formation of basalt, dolerite and gabbro (6 %), polymetamorphic rocks (6 %) and alluvia (4 %) (Figures 1-a and 1-b). The relief and the geology control the spatial distribution of permanent vegetation covering 96 % of the catchment surface area. Shrubland (35 %) and savannah (8 %) are found on peridotite massifs whereas the flatter volcano-sedimentary formations are mainly covered with forests (37 %) and bushland (17 %) (Alric, 2009). Nevertheless, this permanent vegetation cover, which represents the main land use of the Thio River catchment, can be degraded *inter alia* by the development of nickel mining activities (Barselo, 1988). These open-mining casts are either active (*i.e.* Thio Plateau, Camp des Sapins since 1920) or abandoned (~12 sites, from the end of the 19th century to the 1970s, 21% of the catchment area) (Figure 1-c).

The removal of vegetation related to these mining activities increase soil erosion already exacerbated by the island's tropical climate, which is characterized by the succession of a hot wet season (November-April; mean temperature of 27 °C) and a cooler dry season (May-October; mean temperature of 20 °C). Furthermore, cyclones and tropical depressions occur frequently (i.e. every 2.7 years on average). These extreme rainfall events may supply more than 20 % of the annual rainfall (average: 1620 mm; Météo France) and may cause overbank peak flow. The Thio River catchment's river network is particularly reactive to heavy rainfall as most of the 12 tributaries flowing into the main stem of the Thio River (28 km long, Figure 1-b) are governed by a torrential regime (Dubreuil, 1974). In addition, the occurrence of 6 km² of mining roads (Garcin et al., 2017) plays a paramount role in connecting mining zones devoid of vegetation to the river network (Alric, 2009). In general, extensive erosion processes are evident across the Thio River catchment, including rills, gullies, landslides and channel bank erosion (Danloux, 1991). The drainage area of the mining tributaries covers 60% of the Thio River catchment surface area compared to 40% for the non-mining tributaries.

2.2. Sediment sampling

2.2.1 Sediment sources

Source samples were collected after two major floods (characterized by a ~10 year return period): (1) the tropical depression of February 25, 2015 with lag deposits sampled between April 30 and May 5, 2015 (n= 21) and (2) Cyclone Cook on April 10, 2017, sampled between May 16 and 17, 2017 (n= 4). At each sampling site, between five to ten subsamples of fine sediment were collected across a 10-m² surface with a plastic trowel at exposed subaerial sites free of vegetation on channel bars. The subsamples were composited into one sample representative of the fine sediment deposited on the channel bars. In total, 16 samples were collected in tributaries with mining activities (*i.e.* mining tributaries), and eight samples were collected in tributaries draining areas devoid of mining activities (*i.e.* non-mining tributaries) (Figure 1-c). Source samples were oven-dried at 40°C for ~48 hours and sieved successively to 1 mm and 63 µm.

2.2.2 Sediment core

A 1.62 m depth sediment core was collected with an auger in the floodplain (latitude: 21.6357 (South); longitude: 166.1967 (East)) in April 2016 (Figure 1-c). The sediment core was sampled on private land where the owners confirmed the systematic overflow of the river at this location during the largest floods. There was no evidence of bank erosion in the vicinity of the coring site with field observations or aerial imagery taken between 1943 and 2019. The core was cut into sections of variable thickness (n = 32, between 2.5-7 cm, S1 to S32, from top to bottom) to best coincide with the contrasted sediment layers characterized by different colours and textures. Sediment core samples were also oven-dried at 40°C for ~48 hours and sieved successively to 1mm and 63 µm.

2.3. Sediment analyses

2.3.1 Particle size

Laser particle size measurements were conducted on the <1 mm fraction both source and sediment core samples (n= 57) with a Hydro 2000G particle sizer (Malvern) at the Laboratoire Environnement Ville et Société (EVS, Lyon, France). Destruction of the sediment organic matter was performed with a H_2O_2 solution. Laser particle-size measurements were carried out using water as a dispersant. The degree of obscuration ranged between 12–30%. To control the dispersion of samples, stirrer and pump settings were fixed to 750 rpm and 1875 rpm, respectively.

2.3.2 Spectrocolorimetry

Spectrocolorimetric measurements were conducted at the Institut des Géosciences de l'Environnement (IGE, Grenoble, France). The <63µm fraction of all sediment samples were stored in 60 mL polystyrene tubes and analyzed by a portable diffuse reflectance spectrophotometer (Konica Minolta 2600d). Sample quantity varied between 0.1 g and 4 g. Owing to the rather small measuring area (i.e. 3-mm radius circle), and to take into account the possible heterogeneity within the samples, three measurements were taken on each sample. Spectral reflectance was measured between 360 and 740 nm with a 10-nm resolution. All measurements were taken with the D65 standard illuminant, the 10° angle observer and with the specular component excluded. Raw data collected were the spectral reflectance percentage for each of the 39-wavelength classes. From these raw data, three components of various colorimetry models were also derived (Rossel et al., 2006). The standardized tri-stimuli were then converted into CIEL*a*b* cartesian coordinate systems using the equations provided by CIE (1994). The spectrophotometer was calibrated before each set of measurements by making a zero and a white calibration. Control measurements were also taken regularly during and at the end of each set of measurements; the latter consisted of measurements

on red, green and yellow panels as well as six contrasting soil samples. Among the colorimetric parameters analyzed, one of them, a*, was preferentially used to describe the sediment core: when a*< 0, colour of the sediment tends to be green whereas when a*> 0, it tends to be red. First Derivative reflectance of the Visible Spectra(FDVS) was also carried out in order to identify potential differences in the sediment mineralogical composition (Debret et al., 2011).

2.3.3 Elemental geochemistry

The contents of 11 geochemical elements (*i.e.* Mg, Al, Si ,K, Ca, Ti, Cr, Mn, Fe, Ni and Zn) were measured by energy dispersive X-ray fluorescence spectrometry (Epsilon 3, Malvern PANalytical) in source samples (n=16) and sediment sections (n=32) at the Laboratoire des Sciences, du Climat et de l'Environnement (LSCE, Gif-sur-Yvette, France). Calibration curves for the geochemical elements of interest have been established based on 16 certified reference samples including Internal Atomic Energy Agency (IAEA) standards. To conduct these analyses, small mass holder (SMH) cells characterized by an air double X-ray Mylar film were prepared with a sample quantity between 0.2 and 0.5 g of the previously sieved (<63 µm) material. This analysis consisted of irradiating samples with a primary beam generated by an Rh anode X-ray tube emitting electromagnetic waves between 100eV and 1MeV with a maximum power, typical current and voltage fixed to 15 W, 3mA and 50 kV respetively. The associated Si-drift detector had a Be window thickness of 8 µm and recorded the sample spectrum in a 2D optical geometry configuration. X-ray intensities were converted into concentrations using the Epsilon 3 software program through the application of the fundamental parameters method. Correlations between the determined and the standard elemental contents were comprised between 0.90 And 0.99. To validate the calibration, 3 certified standards different from those used for the calibration were analysed, and the associated mean relative error was 17% (SD 5%).

2.4. Identification of sediment layers

Sediment deposits were identified from visual observations of the colour shades and particle size. In addition, four colorimetric, geochemical and particle size parameters were used to corroborate the visual observations and identify sediment deposits that were not visually observable: a*, FDVS, Ni content and the silt-sized fraction.

2.5. Methodological framework for sediment fingerprinting.

Fallout radionuclides (Evrard et al., 2020; Evrard et al., 2015; Wallbrink et al., 1998), geochemical (Collins et al., 1997; Laceby and Olley, 2015) and mineral properties (Klages and Hsieh, 1975; Walden et al., 1997) are the most frequently used tracers to quantify sediment source contributions. More recently, alternative sediment fingerprinting techniques have been developed based on the analysis of properties such as sediment color (Legout et al., 2013; Poulenard et al., 2009), Compound-Specific Stable Isotopes – CSSI signatures (Reiffarth et al., 2016) or environmental DNA (Evrard et al., 2019; Ficetola et al., 2018).

In New Caledonia, a sediment fingerprinting approach had previously been developed to quantify sediment source contributions over two cyclonic events (Sellier et al., 2020). In this approach, the use of geochemical elements such as K to trace mining versus non-mining tributary contributions is supported by the characteristics of the lithological material where both source types are found. Indeed, peridotite massifs where nickel ores are extracted are depleted in K. On the contrary, volcano-sedimentary formations devoid of mining exploitation sites are naturally enriched in K (Sevin, 2014). As mining sites are concentrated in peridotite massifs, the application of this tracer for identifying the mining basin source contribution is straightforward. However, this technique was only applied to sediment collected after cyclones that occurred in 2015 and 2017, and the mining source contributions estimated based on their analysis cannot be extrapolated to the entire period of mining exploitation that started in the 19th century. A sediment tracing approach was therefore

carried out to select the optimal suite of tracers that discriminate mining and non-mining tributary contributions among 11 geochemical properties.

2.5.1. Source discrimination

The sediment fingerprinting technique relies on the ability of tracers to discriminate between sediment sources while remaining conservative (Collins et al., 1996). A range test was applied to ensure that the sediment core samples plotted within the source range (*i.e.* between minimum and maximum values found in source samples). Thereafter, the Mann-Whitney U-test (α= 0.05) selected parameters that significantly discriminated between the two potential sediment sources (*i.e.* mining and non-mining tributaries) for each group of potential tracers. A stepwise discriminant function analysis (DFA) was then used to select the optimal number of potential tracers through the selection of those that collectively maximize the discrimination between both sediment sources for each set of tracers. The optimal tracers for modelling were selected by minimizing the Wilks' lambda values in the backwards mode, with a $p>0.05$ used to select a tracer and $p<0.05$ used to remove a tracer.

2.5.2. Distribution modelling

A distribution modelling approach was used to model the source contributions from the mining and non-mining tributaries to target sediment core samples (Laceby et al., 2015; Laceby and Olley, 2015). This approach incorporates distributions throughout the entire modelling framework, including the source contribution terms and the target sediment. For this two-source model, it is assumed that sediment samples constitute a discrete mixture of their sources, with the contribution from Source A being x, and the contribution of Source B being (1−x) where:

$$Ax + B(1 - x) = \mathrm{C} \quad \text{Equation 1}$$

Where C is the sediment core sample distribution, A and B are again the two source distributions (*i.e.* mining and non-mining tributaries), and x is modelled as a truncated normal

distribution ($0 \leq x \leq 1$) with a mixture mean (μ_m) and standard deviation (σ_m) (Laceby and Olley, 2015).

The model is solved by minimizing the median difference between the distributions of both sides of Equation 1 (C and Ax + B (1 − x)) with the Optquest algorithm in Oracle's Crystal Ball software with a randomly generated mixture mean (μ_m) and standard deviation (σ_m). Source contributions (x) were determined by simulating all distributions in Equation 1 with 2500 Latin Hypercube samples from 500 bins and varying the mixture mean (μ_m) and standard deviation (σ_m). This simulation and solving procedure repeated 2500 times and the median proportional source contribution from these 2500 additional simulations being reported as the source contribution to the target sediment. Uncertainty was determined through summing three quantifiable model uncertainties: (1) the median absolute deviation of the individual source median contribution for the additional 2500 simulations; (2) the modelled standard deviation; and (3) the median absolute deviation of this modelled standard deviation for the 2500 model additional simulations (Laceby et al., 2015).

2.6. Source contribution variability and definition of sediment core units

A statistical analysis based on cumulative deviations, developed by Craddock (1979) and Buishand (1982), was applied to identify the main changes in mining source contributions within the sediment core. This is more specifically a test of data homogeneity based on rescaled adjusted partial sums S^{**}_k:

$$S^{**}_k = \frac{\sum_{i=1}^{n=32}(Yi-Y)}{\sigma}$$

Where Y_i is the mining source contribution of the core section i (S_i), Y is the mean mining source contribution over the entire sediment core and σ is the standard deviation associated with Y. The confidence bound was set at 99 % which determined the critical value of 1.46 and a threshold value (*i.e.* 1.46 x $\sqrt{n}$) of 8.46. If S^{**}_k is lower than the threshold value (*i.e.* 8.46) then mining source

contributions are considered to remain homogenous over the entire sediment core section. On the contrary, if S^{**}_k exceeds the threshold value then mining source contributions are considered heterogeneous and consequently, several sediment units can be defined.

2.7. Establishing core chronology

2.7.1. ^{137}Cs and $^{210}Pb_{xs}$ dating models

Fallout radionuclides (*i.e.* ^{137}Cs, $^{210}Pb_{xs}$) were measured in source (n=24) and sediment core (n=32) samples by gamma spectrometry using coaxial HPGe detectors (Canberra/Ortec). For the measurement of radionuclides in each sample, approximately 1 g of material packed in 15 mL polyethylene containers was analyzed. Indeed, the potential application of fallout radionuclides (*i.e.* ^{137}Cs and $^{210}Pb_{xs}$) for dating overbank sedimentation on the floodplain was demonstrated in numerous studies (Collins et al., 1997; Foucher et al., 2014; Owens et al., 1999). The depth at which the ^{137}Cs peak concentration occurs can be related to the period of peak fallout (*i.e.* in 1965 in the Southern Hemisphere (Turney et al., 2018)) while He and Walling (1996) showed that the exponential radioactive decay of $^{210}Pb_{xs}$ with depth may be used to calculate the mean sedimentation rates over the last 100 years.

2.7.2. Rainfall-runoff analysis

Eight rainfall stations managed by Météo France (*i.e.* Thio Plateau, Thio village, Camps des Sapins) and by Direction des Affaires Vétérinaires Alimentaires et Rurales (DAVAR) (*i.e.* Kouaré, Bel-Air, Ningua, Kuenthio, Mont Do) have daily precipitation records since 1952. Daily discharge has been monitored at a river gauging station located on the main stem of the Thio River section (at Saint-Michel) since 1981 by the DAVAR (Figure 1-b). Overbank flood events at the coring site were assessed by Schneider et al. (2018) based on based on 1) the estimation of bankfull discharge (*i.e.* 790 $m^3\ s^{-1}$) at the coring location according to the discharge time serie and recent flood observations (*i.e.* no overflow observed during cyclone Edna in 2014 (788 $m^3\ s^{-1}$) versus occurrence of overflow

after cyclone Cook in 2017 (796 m^3 s^{-1})); 2) the discharge time-series analysis from the DAVAR database (from 1981 to present) to reconstruct the flood chronology over the last 40 years; and 3) an intensity-duration rainfall statistical analysis (from 1952 to 1980) to extrapolate this reconstruction to the previous period between 1952 and 1981. Schneider et al. (2018) estimated the occurrence of flooding at the coring site and cross-validated these results with a historical database of cyclone and tropical depression events provided by Météo France. Moreover, this flood event chronology was cross-validated with the results of a survey conducted among Thio's inhabitants.

3. Results

3.1. Stratigraphy

Sediment deposits were clearly identified from 72 to 87 cm depth (n= 4, sediment layers: S16, S17, S18, S19) and from 102 to 111.5 cm depth (n= 2, S23, S24) (Figure 2-a). The thickness of these deposits varied between 2.5 and 5 cm. Two types of sediment deposits were observed (*i.e.* fine red-orange deposits and brown deposits). Although no other clearly identifiable sediment layers were found in the rest of the sediment core, clear trends in the colour properties were detected. From 0 to 72 cm depth, the sediment had a light red-brown colour. A second sediment unit was observed from 72 to 111.5 cm depth. It comprised both the sediment deposits mentioned above (n= 6, S16, S17, S18, S19, S23 and S24) and a layer of 15 cm of sediment (*i.e.* from 87 to 102 cm depth) where a mixture between fine red-orange and brown sediment was observed. In contrast, the lower part of the sediment core (*i.e.* from 111.5 to 162 cm depth) was dark brown (Figure 2-a).

All sediment core sections showed a* values exceeding 0 (*i.e.* between 7.9 – 16.0), thus indicating a red coloration of the sediment (Figure 2-b). This red coloration was particularly marked from 45 to 93 cm depth with the highest a* values (*i.e.* between 9.3-16). The remainder of the sediment core (*i.e.* from the top to 45 cm depth and from 93 cm depth to the bottom) is characterized by lower values in a* between 7.9-13.2. Ni contents comprised between 2.9 and 15.5 g

358 kg^{-1} varied in a similar way as a* in the sediment core (Figure 2-c). Ni contents were highest (*i.e.*
359 between 3.9 – 15.5 g kg^{-1}) from 45 to 93 cm depth. The lower part of the sediment core (*i.e.* from 93
360 to 160 cm depth) showed the lowest Ni contents, comprised between 2.9 – 6.9 g kg^{-1}. In the upper
361 part of the sediment core (*i.e.* from 0 to 45 cm depth), Ni contents was nearly constant, in the range
362 between 5.9 – 9.2 g kg^{-1}.

363 This red coloration of sediment associated with high Ni contents likely reflects the occurrence
364 of iron oxides (*i.e.* hematite) and oxyhydroxides (*i.e.* goethite), as indicated by Schwertmann and
365 Latham (1986). The FDVS method used to identify the sediment mineralogical composition confirmed
366 this finding by showing that the main differences were found when examining the intensity of
367 spectral signatures of goethite (*i.e.* at 525 nm) and hematite (*i.e.* at 555, 565 and 575 nm) in the
368 sediment core. Figure 2-d showed that the spectral intensities of goethite and hematite suddenly
369 increased from 45 to 93 cm depth. The lower part of the sediment core (*i.e.* from 93 to 160 cm
370 depth) showed low spectral intensities of goethite and hematite compared to those found in the rest
371 of the sediment core. These three parameters showed a similar trend, for instance a modification of
372 sediment composition from 93 cm depth resulting in the appearance of red-coloured, nickel and
373 goethite/hematite-enriched sediment from 93 cm depth to the uppermost sections of the sediment
374 core.

375 ### 3.2. Identification of sediment layers

376 Seven sediment sections (*i.e.* at S7, S13, S16, S18, S20, S24 and S29) were more specifically
377 distinguished with maximum a* values, maximum Ni contents and maximum spectral intensities of
378 goethite and hematite (Figures 2-b, c, d). Among these seven sediment layers, three (*i.e.* S16, S18 and
379 S24) were visually detected and corresponded to fine red-orange sediment deposits (Figure 2-a). By
380 combining visual observations with geochemical and colorimetric analysis results, ten sediment
381 sections (*i.e.* seven fine red-orange and three brown sediment deposits (*i.e.* S17, S19, S23) were
382 more specifically distinguished from the rest of the sediment core (Figures 2-a, b, c).

Among the ten sediment layers identified visually and based on their different colorimetric and geochemical properties, six showed a sudden increase in their silt fraction (*i.e.* 26 %, SD 9 %), the second dominant grain size fraction after the fine sand fraction (61 %, SD 12 %) in the sediment core: S7, S13, S16, S18, S20 and S24 (Figure 2-e, Table 1). These six core sections all corresponded to red-coloured, nickel and goethite/hematite-enriched sediment deposits (Figures 2-a, b, c, d). Conversely, the three brown sediment deposits visually observed in the sediment core were characterized by a minimum silt fraction (Figures 2-a, e). The variations of the silt fraction (*i.e.* extremum) therefore provided a flood layer indicator. As a result, 19 extrema were found in the sediment core (Figure 2-e).

3.3. Sediment tracing

3.3.1 Source conservation and discrimination

Particle size analysis confirmed the occurrence of particle size sorting during erosion and sediment transfer processes. Indeed, sediment core sections had a finer grain size composition than both sources (D_{10}, D_{50} and D_{90}; Table 1). Particle size sorting may be at the origin of the non-conservation of some tracer properties (Laceby et al., 2017). Nevertheless, the previous results obtained in Sellier et al. (2020) demonstrated that 11 geochemical tracers analyzed in the current research were not significantly impacted by particle size effect. According to the range test results, all properties (except Fe) were found to be conservative. Fe contents measured in the sediment core layers were higher than the highest source values (Table 2). Nine of the remaining potential tracers (*i.e.* Al, Ca, Cr, K, Mg, Mn, Ni, Si, Ti) significantly discriminated between the potential sediment sources (*i.e.* Mann-Whitney U-test, $\alpha = 0.05$, p-value <0.1, Table 3). Among them, only K was selected by the DFA to model sediment source contributions from mining and non-mining sources, respectively, with a Wilk's lambda value of 0.1691. As the Wilk's lambda value is the proportion of the total variance due to the error of the source discrimination, K provided an error of 16.9 % and explained approximately 83.1 % of the differences between the sources (Table 3).

3.3.2 Source contribution variability and definition of sediment core units

The results of the mixing model showed that mining tributaries dominated the sediment inputs along the entire sediment core with a mean contribution of 74 % (SD 13 %) (Figure 3). According to the test of data homogeneity, three distinct sediment core units were identified. The first sediment unit extended from 111.5 cm depth to the bottom of the sediment core. This phase was characterized by a mean mining tributary contribution of 59 % (SD 5 %). Except one maximum of mining tributary contributions reached in layer S29 (*i.e.* 136-141 cm depth, 68 %) cm depth, a low variability in terms of source contributions was observed along the first unit (*i.e.* SD 5 %).

The second unit, from 65 to 111.5 cm depth, corresponded to a transitional phase. Indeed, a sudden increase in mining tributary contributions was observed with a mean contribution of 77 % (SD 14 %) (Figure 3). This phase also showed a higher variability in terms of source contributions (*i.e.* SD 14 %). Overall, the mining tributary contribution reached its maximum along the core (97 %) in S18 (*i.e.* 81-84.5 cm depth). Finally, three other secondary maxima of mining tributary contributions were reached in S16 (*i.e.* 72-77 cm depth, 94 %), S20 (*i.e*. 87-93 cm depth, 82 %) and S24 (*i.e.* 107-111.5 cm depth, 69 %) in this second unit.

In the third unit (*i.e.* from 0 to 65 cm depth), mining tributary contributions stagnated with a mean contribution of 80 % (SD 5 %). They therefore remained largely dominant. Although three maxima of mining tributary contributions were reached in S7 (*i.e.* 31-36 cm depth, 83 %), S11 (*i.e.* 50-57 cm depth, 90 %) and S13 (*i.e.* 60-65 cm depth, 92 %), the variability of source contributions remained rather low (*i.e.* SD 5 %).

3.4. Core dating

Dating of the sequence of sediment deposits could not rely on fallout radionuclide measurements as in most previous studies (Collins et al. (1996) and Foucher et al. (2014)). ^{137}Cs activities were lower than the detection limits in 24 sediment sections. The remaining samples

showed ^{137}Cs activities (<1.7 Bq kg^{-1}) were too low to be used for dating because of the absence of a peak or visible trend in the core profile. Similar results were observed for $^{210}Pb_{xs}$ activities with results below the detection limits in 19 core sections and activities between 3-38 Bq kg^{-1} in the remainder of the core, without any visible trend with core depth (data not shown).

Therefore, only a relative deposition chronology based on the correspondence between the floods identified by the rainfall-runoff analysis carried out by Schneider et al. (2018) and the successive layers found in the sediment core was conducted. The rainfall-runoff analysis carried out by Schneider et al. (2018) led to the identification of 14 overflowing flood events that occurred at the coring site since 1952 to 2017 (Table 4). As the core was collected in 2016, 13 flood events were estimated to have deposited sediment in the floodplain at this location since 1950. This analysis is fraught with uncertainty since it is based on extrapolated data (*i.e.* no discharge time-series over the period 1952-1980, only rainfall information, testimonies of local inhabitants and Météo France archives) and recent flood observations to define bankfull discharge (790 $m^3 s^{-1}$).

According to the rainfall-runoff analysis and Thio's inhabitants testimonies, four flood events occurred between 2009 and 2015 (floods 1 to 4; Table 4), which would locate the year 2009 in layer S7 (*i.e.* 31 - 36 cm depth). Dry sediment deposits with a thickness comprised between 4 and 6 cm have been observed during 2015 and 2017 flood events at the coring location. Moreover, the inhabitant mentioned in particular one of 2013 flood events (*i.e.* July 1st, exceptional event because it did not occur during the cyclone season) as having contributed a mud thickness of *ca.* 20 cm. Estimating the deposition of 7 cm-thick sediment layers during individual flood events or a mean deposition rate of 2 cm yr^{-1} appears therefore to be relevant (Figure 4).

The limit between units 2 and 3 (*i.e.* at 65 cm depth) was estimated to occur in 1990 according to the four next overbank floods (Table 4; floods 5 to 8, Figure 4). Among the 13 flood events identified (Table 4) by the rainfall-runoff analysis, Cyclone Alison (1975) triggered massive mining waste transfers through the river systems (Garcin et al., 2017; Gosset, 2016). Based here again only

on the relative deposition chronology, this tipping point should correspond to S15 *(i.e*. from 69 to 72 cm depth), in unit 2 (Figure 4). This hypothesis remains consistent because it leads this exceptional event to be comprised in unit 2 which is also a transition phase and where a significant increase in the contribution of mining tributaries was observed. However, all the results originating from the sediment tracing approach, colorimetric and geochemical analyses converged and indicated that this flood likely corresponds to S18 (*i.e.* from 81 to 84.5 cm depth), also located in unit 2. Indeed, the maximum of mining tributary contributions was reached in this sediment section (S18, 97 %, Figure 4). S18 is also characterized by the stronger red coloration of sediment (*i.e.* highest a* values), highest Ni contents and highest spectral intensity of iron oxides and oxy-hydroxides (Figures 3-b, c, d). It is very likely that several floods have not been recorded in this study due to uncertainties in the analyses (*i.e.* extrapolated data, parameter estimation based on recent flood event observations, core cutting), thus explaining this light temporal shift. Nevertheless, the location of this flood in the transition phase (*i.e.* unit 2) suggests that the relative deposition chronology is consistent. Moreover, we obtained a 1957 deposition year for S22 (*i.e.* from 97 to 102 cm depth) which is again consistent with the assumption that the 1950s sediment deposits would correspond to those layers located below 111.5 cm depth (*i.e.* a change between units 1 and 2) (Figure 4).

4. Discussion

4.1. Sediment sources variability and the mining history of the Thio River catchment (1880 – 2016)

The sediment core has been divided into three main units in terms of sediment source contributions (Figure 4): (1) unit 1 (before ~1950), the contributions of the mining tributaries are high, and remain relatively constant with time: 59 % (SD 5 %); (2) unit 2 (~ 1950 – 1990) demonstrates a high variability and overall a rapid increase of these latter (*i.e.* mean of 77 %, SD 14 %) ; (3) unit 3 (~1990 – 2016), the mining tributary contributions are 20 % higher than in unit 1 with

low variations (*i.e.* 80 %, SD 5 %). These sediment deposit units can now be compared with the mining history of New Caledonia in general, and the Thio River catchment in particular.

4.1.1. Period 1, from 1880 to 1950: the manual handling mining without any environmental legislation

The first period *(i.e.* 1880s-1950s) corresponds to the beginning of mining activities in New Caledonia. As shown in Figure 5, nickel ore production by manual handling mining was very low (*i.e.* around mean 30 000 tons per year) during this period. The recent discovery of nickel ores in 1864 and the associated need to find suitable smelting processes as well as the employed extraction process (*i.e.* manual extraction) may explain this low nickel ore production. Furthermore, at this time, mining colonial companies focused mainly on the extraction of the most nickel-rich ores (*i.e.* saprolites), which delineated the extent of mining sites.

This period would correspond to unit 1 (*i.e.* from 111.5 cm depth to the bottom) observed within the sediment core. Despite the limited mining development and the manual extraction, the contribution of mining tributaries was high *(i.e*. 59 %, SD 5 %) (Figures 4 and 5). Accordingly, this past activity left a strong imprint in the landscape and has driven and probably still significantly drives the exports of suspended sediment to the delta and the lagoon. Mining contributions were expected to dominate because peridotite massifs, once exploited, represent the most erosion-sensitive structures (Dumas, 2010). It is only with the increasing scarcity of saprolite ores that the mining industries began to change their methods of extraction. The 1920s marked open-cast nickel mining implementation to facilitate extraction of saprolite ores located at depth (Figure 5).

4.1.2. Periods 2 and 3, from 1950 to 1989: the mechanization of mining activities, from a non-regulated extraction to the first environmental regulations

For the second period initiated in 1950s, the mechanization of mining activities began with the excavators, bulldozers and caterpillars left in New Caledonia by the US Army Forces after the

505 Second World War which helped make it possible to increase nickel ore production by a factor of 7.
506 The huge development of mining industry in New Caledonia occurred mainly in the Thio River
507 catchment. In the absence of environmental legislation, the sensitivity of soils to erosion increased
508 extensively in the Thio River catchment during this period, as a consequence to (1) the increasing
509 bare soil surface area (233 ha to 775 ha, factor 13 from ~ 1950 to 1975), (2) the rapid extent of
510 mining prospect roads (44 ha to 613 ha, factor ~ 4 from ~ 1950 to 1975) and (3) the direct dumping
511 of mining waste rocks on the hillslopes (4 to 30 million tons from ~ 1950 to 1975) (Garcin et al.,
512 2017). Indeed, the rapid increase of nickel ore production was accompanied by a sharp increase in
513 mining waste (*i.e.* 2.1 tons per tons of nickel ore mined; Iltis (1992); Figure 5), resulting in an increase
514 of sediment inputs to the New Caledonian rivers (Bird et al., 1984; Iltis, 1992).

515 Cyclone Alison occurred in 1975, after the huge development of an unregulated mining
516 industry and an 8-year period of very low cyclonic activity (Table 4). Among the 13 flood events
517 identified (Table 4), Cyclone Alison (1975) was mentioned repeatedly by the inhabitants of Thio as
518 the event that triggered the first significant problems of overburden and hypersedimentation in the
519 river systems. Garcin et al. (2017) showed that overburden material was stored on the mine foothills
520 prior to 1975 and Cyclone Alison was a major contributor to the dumping of this mining waste into
521 the river systems. Indeed, Cyclone Alison began to connect the sedimentary sources (*e.g.* mining
522 areas, waste dumps, prospecting roads) to the creeks and the Thio delta.

523 Cyclone Alison was concomitant with the establishment of environmental legislation in France
524 and New Caledonia (environmental code, n°75-633/1975) that prohibited the disposal of waste
525 products and the recovery of materials, including the prohibition of direct dumping of mining waste
526 rocks on the hillslopes. The polluter pays principle was then applied for the mining extraction from
527 1975. However, in the case of the Thio River catchment, nearly a century of non-regulated mining
528 activity had already led to severe environmental impacts that an environmental law could hardly
529 regulate, especially during a huge event such as Cyclone Alison.

530 Regarding the sediment core analysis, periods 2 and 3 (1950 – 1989) would correspond to unit
531 2. During these periods, a sudden increase in the contribution of mining tributaries was observed (*i.e.*
532 mean of 77 %, SD 14 %). Moreover, visual observations, colorimetric and geochemical analyses
533 indicated a modification of sediment composition during this phase resulting in the dominance of
534 red-coloured, nickel and goethite/hematite-enriched sediment. This red coloration of sediment
535 described in the studies (Bird et al., 1984; Iltis, 1992) but also observed in the sediment core could
536 correspond to the release of laterites initially stored on the foothills.

537 Moreover, this variability of mining tributary contributions observed in unit 2 could be
538 explained by the gradual transformation of landscapes, for example the opening of new mining
539 concessions, the mining dumps on hillslopes, the exploration of new mining sites requiring the
540 creation of mining roads. The high variability of mining tributary contributions at the outlet could
541 also be attributed to 1) a low hydro-sedimentary connectivity and 2) a spatial variability of rainfall
542 that can locally modify the contributions of sediment sources already identified in Sellier et al.
543 (2020). As the mining activity areas increase, so does the probability that a tropical cyclone or
544 depression will affect one of these areas and connect these different sources to the creeks.

545 ### *4.1.3. Period 4, from 1989 to present: a period of industrial extraction with an increasing*
546 ### *concern of environmental issues by policies and mining industries*

547

548 Since 2009, a Mining Code in New Caledonia regulates the present mining activities (*i.e.* post-
549 1975) (Figure 5). Among other points, it focused on water pollution in the Thio River and its lagoon
550 with suspended sediment supplied by mining areas in activity. It requires the implementation of
551 mitigation infrastructures on mining areas and environmental monitoring, for instance the collection
552 of rainwater and suspended sediment on mining areas, the sedimentation of fine particles in

553 retention ponds, the stabilization of hillslopes and the planting of vegetation in abandoned mining
554 areas.

555 The relative deposition chronology made it possible to locate this period within the sediment
556 core. Unit 3 corresponds to period 4 (*i.e.* 1990-2016, with 8 flood events). Mining tributaries
557 dominated the sediment input with a mean contribution of 80 % (SD 5 %) (Figure 4). Since this date,
558 the hydro-sedimentary connectivity is very high. This could explain in particular the low variability of
559 mining tributary contributions in phase 3 (*i.e.* SD 5 %) where finally, present and past mining industry
560 drives most of the soil erosion in the entire catchment.

561 ### 4.2. The tipping point concept applied to the Thio River hydro-sedimentary
562 system

563 Despite the efforts made to reduce the environmental impacts of mining activities since
564 1975, sediment transiting the river system still mainly originates from mining areas. The soil erosion
565 processes occurring in peridotite massifs, once initiated, are difficult to contain. The hydrosystem has
566 experienced a shift to another erosive state during the 1950-1989 period, and the year 1975, with
567 the occurrence of Cyclone Alison, can be considered as a tipping point. The concept of tipping point
568 reflects the idea of a change of state of a system with feedback loops that propel the system on a
569 completely new course (Scheffer et al., 2001). This concept seems to be well adapted to the hydro-
570 sedimentary system of the Thio River catchment.

571 The results derived from the sediment core analysis show that rehabilitation and soil erosion
572 mitigation infrastructures and initiatives did not allow a quick recovery to a pre-1950s state (*i.e.* unit
573 1). A slow trend in the decrease of the mining fraction has been recorded in unit 1 since 2009 (from
574 83 % to 70 %). However, the results obtained based on the analysis of the sediment deposits
575 collected after Cyclone Cook in 2017 in Sellier et al. (2020) show that these management structures
576 are not sufficiently effective during intense tropical cyclones (88 % of mining tributary contribution in

2017). This conclusion is consistent with measurements conducted downstream of retention ponds during an extreme event in 2001 in another mining location in New Caledonia (Mathys et al., 2015). Indeed, the impoundments and runoff control infrastructures are effective only for floods with limited return periods, for instance hourly rainfall intensity less than 2 years return-period.

However, the control of erosion occurring in active mining tributaries is probably masked by the contribution of the legacy mining sources that remain very active. In 1950, the mining contribution was on average 60 %, for instance three quarters of the present mining tributary contribution. Unfortunately, the sediment tracing approach did not discriminate between legacy and current mining contributions. The destabilization of the hillslopes, the difficulties to reduce the sediment loads during cyclonic events on active mining areas, and the presence of fine sediment in all river compartments are so high that it is very likely that a recovery to a pre-1950s state will not be possible without a strong human intervention, for example re-vegetation, runoff and waste water management, along with hillslope stabilization. Moreover, long-term surveys of mining tributary contributions and sediment loads during each cyclone is required to monitor the evolution of sediment source contributions in the coming years and to assess the efficiency of re-habilitation works.

4.3. Comparison with literature studies on legacy sediment

Similar cases have been observed in the literature around the world. The term 'legacy sediment' in particular has appeared in the literature since the 1980s and is defined as sediment deposits episodically produced by accelerated erosion associated with intensive anthropogenic activities (*e.g.* agriculture, mining; (James, 2013). In a mining context, Macklin (1985) showed that the intensification of mining activities (*i.e.* 1858-1908) had significantly contributed to sediment inputs in the River Axe catchment (Britain). Indeed, floodplain sedimentation rates were four times higher during this period (*i.e.* 1858-1908) compared to those recorded during the period when mining activity had ceased (*i.e*. after 1908). This legacy sediment can be identified in particular by

significantly higher metal contents than those recorded in the pre-mining state in a sediment sequence (Brunskill et al., 2004; Ciszewski et al., 2012; Lecce and Pavlowsky, 2001). However, a gap between a period of increased mining activity and the resulting pollution may also occur several years or even several decades later as observed by Nguyen et al. (2009). Indeed, the authors showed that owing to the absence of environmental legislation to manage mining waste during rapid industrialization periods (*i.e.* 1950s-1960s), high contents of heavy metal were recorded over the period 1975-1990 in a lacustrine core in Hungary. Valette-Silver (1993) compiled surveys about heavy metal contamination associated with the industrialization period (*i.e.* 1960s-1970s) and focused on the effect of implementation of new discharge and emission regulations from 1980s on concentration trends in sediment cores. Results showed that a decrease in heavy metal contents was observed in sediment without returning to the pre-mining state. Indeed, this legacy sediment (*i.e.* mining waste and mining alluvial sediment) is not permanently stored and is therefore likely to be gradually remobilized (Coulthard and Macklin, 2003).

4.4. Implications for tracing the impact of mining activities on sediment supply in the South Pacific

One objective of the current research was to apply a sediment fingerprinting approach that had previously been used to trace sediment sources over two cyclonic events to a sediment core covering several decades. The geochemical properties used in this approach were shown not to be impacted by particle size effect (Sellier et al., 2020). This study showed that most of them (*i.e.* Mg, Al, Si ,K, Ca, Ti, Cr, Mn, Ni, and Zn) remained conservative over time. Among these latter, K offered the best discrimination between sediment sources. It is a lithological tracer that discriminates the sediment contributions of volcano-sedimentary formations that of peridotite massifs where mining sites are located. The results obtained with the K-model showed that mining contributions dominate sediment input are corroborated by the remote sensing study conducted by Garcin et al. (2017). The authors showed in particular that natural erosion of peridotite massifs represented approximately 12

% of the sediment production areas in 1954 (*i.e.* beginning of mechanization of mining activity), 5 % in 1976 and 2008. As a result, mining erosion is largely dominant on peridotite massifs (*i.e.* ~95 %). Therefore, the results demonstrated that the contributions of mining tributaries provided the main sediment source in the Thio River catchment. This tracer is therefore just as effective to quantify the contributions of sources associated with recent events (Sellier et al., 2020) as it is over longer periods of time.

4.5. Difficulties and limitations of sediment core sampling

The deposition rate determined in this study (*i.e.* mean annual deposition rate of 2 cm yr^{-1}) cannot be considered as representative of the sedimentation rate observed across the entire watershed. Lecce and Pavlowsky (2001) and Knox (2006) showed in particular that deposition rates were higher in the floodplain than in upper catchment parts. Furthermore, successive sediment deposits recorded at one location in the floodplain cannot be considered representative of the sediment deposits across the entire deltaic floodplain. Lecce and Pavlowsky (2001) and Knox (2006) insisted on the notion of topography: deposition rates were the highest on the lowest valley floor surfaces. Calhoun and Fletcher III (1999) also showed in a subtropical, heavy rainfall, steep-sided catchment (*i.e.* Hanalei, Kauai; Hawaï Islands) that distance from the river is also a factor influencing sediment deposition. They observed decreasing sediment deposition rates with increasing distance from the main river channel. The more recent study conducted by Omengo et al. (2016) in a tropical floodplain (*i.e.* Tana River, Kenya) confirmed these results and showed that during flood events, sediment settles rapidly and its transport to remote parts of the floodplain remains very limited.

Future studies could be devoted to the analysis of several other sediment profiles coupled with geophysical measurements (*e.g.* LIDAR) at the level of the deltaic floodplain of the Thio River catchment in order to have a better spatial and temporal representativity of the sediment deposits. However, given the location of the sediment core sampled in this study (*i.e.* 10 m from the river, at

651 the mouth of the deltaic floodplain), it is likely that the deposition rate determined is representative
652 of the upper limit of the sedimentation rates that may occur in this floodplain.

653 ### 4.6. Fine and coarse sediment transport: distinct sources and dynamics

654 The observations made in this study only focused on the dynamics of the finest fraction of
655 sediment (i.e. <2 mm). Hence, these results cannot be extrapolated to coarse sediment transport (*i.e.*
656 >2 mm) as they are characterised by very different sediment sources and dynamics. Both type of
657 sediment are thus implying very different management.

658 Sources of coarse sediment are mainly limited to legacy sediment (*i.e.* inherited mining waste)
659 and landslides (*i.e.* triggered on mining or non-mining areas). Because of the sudden decrease of the
660 channel slope, this coarse sediment deposited mainly in the creeks upstream the confluences with
661 the Thio River. On the contrary, the sources of fine sediment are rather much more diffuse at the
662 catchment scale with the erosion of mining sites, mining prospection areas, mining roads, inherited
663 mining waste (mining sources) and erosion of large bare soil surfaces generated by fires, landslides or
664 trampling (non-mining sources). As a consequence, this sediment fraction can easily reach the
665 lagoon, even during low flood magnitude, and deposits all along the drainage network and the delta.

666 Severe aggradation of mining tributaries by coarse sediment occurred from the start of mining
667 activities and it intensified following the partial destocking of inherited mining waste generated by
668 the occurrence of cyclone Alison in 1975. Since this event and following the implementation of
669 mitigation infrastructures on the tributaries, the processes of creek aggradation tend to decrease
670 (Garcin et al., 2018). In contrast, fine sediment transport from mining sources does not show any
671 trend of decrease, despite the rehabilitation efforts and the construction of retention basins to
672 mitigate fine sediment transfer.

673

5. Conclusions and perspectives

The current study has reconstructed the temporal evolution of the sediment source contributions based on the analysis of a sediment core collected in the alluvial plain at the outlet of the Thio River catchment. Mining contributions have dominated and continue to dominate sediment inputs to the river systems (74 %, SD 13 %). The past activity has left strong imprints across the landscape. Despite the limited mining development and the manual extraction, the contribution of mining tributaries during the pre-mechanization period (<1950) was found already very high (*i.e.* 59 %, SD 5 %). These contributions sharply increased during the period of mechanization (1950s-1975) (*i.e*. increase of 18 %). The absence of environmental legislations has led to the storage of millions of tons of mining waste on the foothills. It was only during a particularly intense rainfall event (*i.e.* Cyclone Alison in 1975) that this mining waste, accumulated over 25 years, was dumped into the river system. At present, this de-stocking is still ongoing almost 45 years after the triggering event. Despite the entry into force of environmental protection legislation in 1975 that prohibited sediment storage on the foothills and the more recent 2009 mining code that initiated the installation of control measures to limit runoff and erosion on-site (*e.g.* retention ponds, waste water management), mining tributary contributions remained very high (80 %, SD 5 %), raising questions about the effectiveness of the expensive hydraulic infrastructures to deal with the extreme rainfall events.

This study thus illustrates the challenging problem of environmental pollution legacy. This issue is critical and raises many questions about the current and future responsibilities of the mining industries since the polluter pays principle would imply that the mining industries should pay for the pollution that they have generated since 1975. However, it remains difficult to quantify unambiguously the fraction of pollution that is attributed to present and past activities. Furthermore, a better distinction between the legacy sediment and the waste mining sediment would also help guiding the implementation of effective mitigation measures. Many mining sites have been

699 abandoned since the 1970s and most of them have not been rehabilitated yet (*e.g.* re-vegetated);
700 they may therefore contribute significantly to the sediment inputs into the river systems. In such a
701 context, the increased mining extraction observed during the last decade should be accompanied by
702 huge efforts of rehabilitation and the installation of runoff mitigation infrastructures in both
703 abandoned and operational mining sites.

704 However, according to the tipping point theory (Scheffer *et al.*, 2001), a return to a pre-mining
705 state is unlikely, even illusory. Indeed mitigating efforts should be significantly greater than the
706 extractive forces that have created this situation during the last 150 years. Mining is, and will remain
707 part of the Thio River catchment's landscape for centuries. This perspective raises tensions between
708 the local population, the mining industries and the government. Local residents are suffering daily
709 from the deleterious impacts of floods, soil and water pollution. They are now waiting for effective
710 solutions to be implemented. A pragmatic approach should be defined in close consultation with the
711 population, the levels of pollution that would be acceptable locally according to local environmental,
712 economic and societal issues. At strategic locations, significant rehabilitation efforts should be made
713 for limiting pollution allowing for the development of alternative economic activities (*e.g.* agriculture,
714 tourism) and the well-being of inhabitants.

715 Since by definition, mineral resources are not renewable, this study finally addresses a major
716 socio-environmental issue for the post-mining period that will come one day. Hydraulic
717 infrastructures that limit runoff and sediment transfer runoff have limited lifetimes. If they are no
718 longer properly managed and maintained, important risks of reservoir failing and landslide can occur
719 with disastrous environmental, economic and social injuries during cyclonic events. Accordingly, in a
720 post-mining perspective, when the mining sites will close, who will control and maintain these
721 mitigation runoff infrastructures (*e.g*. roads drainage, retention and infiltration basins) day after day,
722 who will pay for it, and finally for how long (several decades at least, centuries)?

Hence, a thorough understanding of past, present and future sediment dynamics in the mining catchments is required to guide decision-making in these mining environments. A study of the biophysical processes (*e.g.* sediment transfer mechanism and vegetation recovery) and the social processes (representation of mining and its impacts by the different actors) have to be conducted together because all these aspects are strongly interconnected. This sediment tracing study contributes to improve this understanding and could also contribute to provide a method to evaluate the long-term efficiency of solutions for preventing erosion in mining areas. This multi-proxy approach could be extended to other mining catchments of New Caledonia but also to other similar mining catchments around the world (*e.g.* Australia, Brazil, Dominican Republic, Cuba).

Acknowledgements

The PhD fellowship of Virginie Sellier was funded by the 'Commissariat à l'Energie Atomique et aux Energies Alternatives' (CEA, France). Research was supported by the CNRT – Nickel and Environment programme (IMMILA, 'de la mine au lagon', n°10PS2013-CNRT.UNC/IMMILA). The authors are grateful to Vincent Gaertner for the analyses at the research platform OMEAA-CNRS, Louise Schneider (whose master traineeship fellowship was funded by Labex IMU ('Intelligence des Mondes Urbains') as well as to Jean-Guy M'Bouery, Pierre Chanel, Jean-Jean, Lorenza M'Bouery, Nicolle Mathys for their invaluable support to identify and have access to the field sampling sites.

6. References

Alric, R., 2009. Recueil des débits caractéristiques de la Nouvelle Calédonie. Direction des Affaires Vétérinaires Alimentaires et Rurales (DAVAR). Service de l'eau des statistiques et études rurales. Observatoire de la ressource en eau Nouméa.

Amundson, R., Berhe, A.A., Hopmans, J.W., Olson, C., Sztein, A.E., Sparks, D.L., 2015. Soil and human security in the 21st century. Science, 348(6235), 1261071.

Bajard, M., Poulenard, J., Sabatier, P., Etienne, D., Ficetola, F., Chen, W., Gielly, L., Taberlet, P., Develle, A.-L., Rey, P.-J., 2017. Long-term changes in alpine pedogenetic processes: Effect of millennial agro-pastoralism activities (French-Italian Alps). Geoderma, 306, 217-236.

Balamurugan, G., 1991. Tin mining and sediment supply in Peninsular Malaysia with special reference to the Kelang River basin. Environmentalist, 11(4), 281-291.

Baltzer, F., Trescases, J., 1971. Erosion, transport et sédimentation liés aux cyclones tropicaux dans les massifs d'ultrabasites de Nouvelle-Calédonie. Cahiers ORSTOM Série Géologie, 3(2), 221-244.

Barselo, P., 1988. Dégradation de la végétation et érosion dans la commune de Thio (Nouvelle-Calédonie).

Bird, E.C.F., Dubois, J.P., Iltis, J.A., 1984. The impacts of opencast mining on the rivers and coasts of New Caledonia. Tokyo, Japan, United Nations University.

Blake, W.H., Wallbrink, P.J., Wilkinson, S.N., Humphreys, G.S., Doerr, S.H., Shakesby, R.A., Tomkins, K.M., 2009. Deriving hillslope sediment budgets in wildfire-affected forests using fallout radionuclide tracers. Geomorphology, 104(3-4), 105-116.

Borrelli, P., Robinson, D.A., Fleischer, L.R., Lugato, E., Ballabio, C., Alewell, C., Meusburger, K., Modugno, S., Schütt, B., Ferro, V., 2017. An assessment of the global impact of 21st century land use change on soil erosion. Nature communications, 8(1), 2013.

Brunskill, G.J., Zagorskis, I., Pfitzner, J., Ellison, J., 2004. Sediment and trace element depositional history from the Ajkwa River estuarine mangroves of Irian Jaya (West Papua), Indonesia. Continental Shelf Research, 24(19), 2535-2551.

Buishand, T.A., 1982. Some methods for testing the homogeneity of rainfall records. Journal of hydrology, 58(1-2), 11-27.

Calhoun, R.S., Fletcher III, C.H., 1999. Measured and predicted sediment yield from a subtropical, heavy rainfall, steep-sided river basin: Hanalei, Kauai, Hawaiian Islands. Geomorphology, 30(3), 213-226.

Ciszewski, D., Kubsik, U., Aleksander-Kwaterczak, U., 2012. Long-term dispersal of heavy metals in a catchment affected by historic lead and zinc mining. Journal of Soils and Sediments, 12(9), 1445-1462.

Collins, A., Walling, D., Leeks, G., 1997. Use of the geochemical record preserved in floodplain deposits to reconstruct recent changes in river basin sediment sources. Geomorphology, 19(1-2), 151-167.

Collins, A.L., Walling, D.E., 2004. Documenting catchment suspended sediment sources: problems, approaches and prospects. Progress in Physical Geography, 28(2), 159-196.

Collins, A.L., Walling, D.E., Leeks, G.J.L., 1996. Composite fingerprinting of the spatial source of fluvial suspended sediment : a case study of the Exe and Severn river basins, United Kingdom. Géomorphologie, 2(2), 41-53.

Coulthard, T.J., Macklin, M.G., 2003. Modeling long-term contamination in river systems from historical metal mining. Geology, 31(5), 451-454.

Craddock, J., 1979. Methods of comparing annual rainfall records for climatic purposes. Weather, 34(9), 332-346.

Danloux, J., Laganier, R., 1991. Classification et quantification des phénomènes d'érosion, de transport et de sédimentation sur les bassins touchés par l'exploitation minière en Nouvelle Calédonie.

793 Danloux, J.L., Richard, 1991. Classification et quantification des phénomènes d'érosion, de transport
794 et de sédimentation sur les bassins touchés par l'exploitation minière en Nouvelle-Calédonie.
795 IRD, Rapports scientifiques et techniques.
796 Dearing, J., Battarbee, R., Dikau, R., Larocque, I., Oldfield, F., 2006. Human–environment interactions:
797 learning from the past. Springer.
798 Debret, M., Sebag, D., Desmet, M., Balsam, W., Copard, Y., Mourier, B., Susperrigui, A.-S., Arnaud, F.,
799 Bentaleb, I., Chapron, E., 2011. Spectrocolorimetric interpretation of sedimentary dynamics:
800 the new "Q7/4 diagram". Earth-Science Reviews, 109(1-2), 1-19.
801 Dubreuil, P., 1974. Initiation à l'analyse hydrologique.(ORSTOM). MASSON & CIE, EDITEURS, 216p.
802 Dumas, P., 2010. Méthodologie de cartographie de la sensibilité des sols à l'érosion appliquée à la
803 région de Dumbéa à Païta-Bouloupari (Nouvelle-Calédonie). Les Cahiers d'Outre-Mer. Revue
804 de géographie de Bordeaux, 63(252), 567-584.
805 Evrard, O., Chaboche, P.-A., Ramon, R., Foucher, A., Laceby, J.P., 2020. A global review of sediment
806 source fingerprinting research incorporating fallout radiocesium (137Cs). Geomorphology,
807 107103.
808 Evrard, O., Laceby, J.P., Ficetola, G.F., Gielly, L., Huon, S., Lefèvre, I., Onda, Y., Poulenard, J., 2019.
809 Environmental DNA provides information on sediment sources: A study in catchments
810 affected by Fukushima radioactive fallout. Sci Total Environ, 665, 873-881.
811 Evrard, O., Laceby, J.P., Huon, S., Lefèvre, I., Sengtaheuanghoung, O., Ribolzi, O., 2015. Combining
812 multiple fallout radionuclides (137Cs, 7Be, 210Pbxs) to investigate temporal sediment source
813 dynamics in tropical, ephemeral riverine systems. J Soils Sediments, 16(3), 1130-1144.
814 Ficetola, G.F., Poulenard, J., Sabatier, P., Messager, E., Gielly, L., Leloup, A., Etienne, D., Bakke, J.,
815 Malet, E., Fanget, B., 2018. DNA from lake sediments reveals long-term ecosystem changes
816 after a biological invasion. Sci Adv, 4(5), eaar4292.
817 Foucher, A., Salvador-Blanes, S., Evrard, O., Simonneau, A., Chapron, E., Courp, T., Cerdan, O.,
818 Lefèvre, I., Adriaensen, H., Lecompte, F., Desmet, M., 2014. Increase in soil erosion after
819 agricultural intensification: Evidence from a lowland basin in France. Anthropocene, 7, 30-41.
820 García-Ruiz, J.M., Beguería, S., Lana-Renault, N., Nadal-Romero, E., Cerdà, A., 2017. Ongoing and
821 emerging questions in water erosion studies. Land degradation & development, 28(1), 5-21.
822 Garcin, M., Gastaldi, Y., Lesimple, S., 2017. Quantification et évolution temporelle des apports
823 miniers dans les rivières calédoniennes. BRGM/RP-66840-FR, 44 p., 23 fig., 5, Bureau des
824 Recherches Géologiques et Minières

825
826 Garcin, M., Richard, D., Liébault, F., Recking, A., Piton, G., Sabinot, C., Worliczek, E., Lesimple, S.,
827 Bertrand, M., Gastaldi, Y., 2018. Gestion du passif de l'activité minière en Nouvelle-
828 Calédonie. Guide méthodologique 2018, CNRT" Nickel et son environnement".
829 Gosset, L., 2016. Rivières engravées à Thio, Nouvelle-Calédonie : vécus et attentes de la population.
830 He, Q., Walling, D., 1996. Use of fallout Pb-210 measurements to investigate longer-term rates and
831 patterns of overbank sediment deposition on the floodplains of lowland rivers. Earth Surface
832 Processes and Landforms, 21(2), 141-154.
833 Hoffmann, T., Thorndycraft, V.R., Brown, A.G., Coulthard, T.J., Damnati, B., Kale, V.S., Middelkoop, H.,
834 Notebaert, B., Walling, D.E., 2010. Human impact on fluvial regimes and sediment flux during
835 the Holocene: Review and future research agenda. Global and Planetary Change, 72(3), 87-
836 98.
837 Iltis, J., 1992. La mine, élement de la controverse écologique dans le Pacifique Sud. L'Espace
838 géographique, 193-205.
839 James, L.A., 2013. Legacy sediment: definitions and processes of episodically produced
840 anthropogenic sediment. Anthropocene, 2, 16-26.
841 Klages, M., Hsieh, Y., 1975. Suspended Solids Carried by the Gallatin River of Southwestern Montana:
842 II. Using Mineralogy for Inferring Sources 1. Journal of Environmental Quality, 4(1), 68-73.

Knox, J.C., 2006. Floodplain sedimentation in the Upper Mississippi Valley: Natural versus human accelerated. Geomorphology, 79(3-4), 286-310.
Laceby, J.P., Evrard, O., Smith, H.G., Blake, W.H., Olley, J.M., Minella, J.P.G., Owens, P.N., 2017. The challenges and opportunities of addressing particle size effects in sediment source fingerprinting: A review. Earth-Sci. Rev., 169, 85-103.
Laceby, J.P., McMahon, J., Evrard, O., Olley, J., 2015. A comparison of geological and statistical approaches to element selection for sediment fingerprinting. J Soils Sediments, 15(10), 2117-2131.
Laceby, J.P., Olley, J., 2015. An examination of geochemical modelling approaches to tracing sediment sources incorporating distribution mixing and elemental correlations. Hydrol. Process., 29(6), 1669-1685.
Lal, R., 1983. Soil erosion in the humid tropics with particular reference to agricultural land development and soil management. Int. Assoc. Hydrol. Sci. Publ, 140, 221-239.
Lecce, S.A., Pavlowsky, R.T., 2001. Use of mining-contaminated sediment tracers to investigate the timing and rates of historical flood plain sedimentation. Geomorphology, 38(1-2), 85-108.
Legout, C., Poulenard, J., Nemery, J., Navratil, O., Grangeon, T., Evrard, O., Esteves, M., 2013. Quantifying suspended sediment sources during runoff events in headwater catchments using spectrocolorimetry. J Soils Sediments, 13(8), 1478-1492.
Macklin, M.G., 1985. Flood-plain sedimentation in the upper Axe Valley, Mendip, England. Transactions of the Institute of British Geographers, 235-244.
Mathys, N., Caze, N., Richard, D., 2015. Guide méthodologique: suivi hydrologique et sédimentaire des petits bassins versants miniers de Nouvelle-Calédonie.
Muchena, F., Onduru, D., Gachini, G., De Jager, A., 2005. Turning the tides of soil degradation in Africa: capturing the reality and exploring opportunities. Land Use Policy, 22(1), 23-31.
Navarro, M., Pérez-Sirvent, C., Martínez-Sánchez, M., Vidal, J., Tovar, P., Bech, J., 2008. Abandoned mine sites as a source of contamination by heavy metals: a case study in a semi-arid zone. Journal of Geochemical exploration, 96(2-3), 183-193.
Nguyen, H., Braun, M., Szaloki, I., Baeyens, W., Van Grieken, R., Leermakers, M., 2009. Tracing the metal pollution history of the Tisza River through the analysis of a sediment depth profile. Water, air, and soil pollution, 200(1-4), 119-132.
Nyman, P., Sheridan, G.J., Smith, H.G., Lane, P.N.J., 2011. Evidence of debris flow occurrence after wildfire in upland catchments of south-east Australia. Geomorphology, 125(3), 383-401.
Omengo, F.O., Alleman, T., Geeraert, N., Bouillon, S., Govers, G., 2016. Sediment deposition patterns in a tropical floodplain, Tana River, Kenya. Catena, 143, 57-69.
Owens, P.N., Walling, D.E., Leeks, G.J., 1999. Use of floodplain sediment cores to investigate recent historical changes in overbank sedimentation rates and sediment sources in the catchment of the River Ouse, Yorkshire, UK. Catena, 36(1-2), 21-47.
Poulenard, J., Perrette, Y., Fanget, B., Quetin, P., Trevisan, D., Dorioz, J.-M., 2009. Infrared spectroscopy tracing of sediment sources in a small rural watershed (French Alps). Science of the Total Environment, 407(8), 2808-2819.
Reiffarth, D., Petticrew, E., Owens, P., Lobb, D., 2016. Sources of variability in fatty acid (FA) biomarkers in the application of compound-specific stable isotopes (CSSIs) to soil and sediment fingerprinting and tracing: A review. Science of the Total Environment, 565, 8-27.
Restrepo, J.D., Kettner, A., Syvitski, J.P., 2015. Recent deforestation causes rapid increase in river sediment load in the Colombian Andes. Anthropocene, 10, 13-28.
Restrepo, J.D., Syvitski, J.P., 2006. Assessing the effect of natural controls and land use change on sediment yield in a major Andean river: the Magdalena drainage basin, Colombia. Ambio: a Journal of the Human Environment, 35(2), 65-75.
Rossel, R.V., Minasny, B., Roudier, P., McBratney, A., 2006. Colour space models for soil science. Geoderma, 133(3-4), 320-337.
Russell, K.L., Vietz, G.J., Fletcher, T.D., 2017. Global sediment yields from urban and urbanizing watersheds. Earth-Science Reviews, 168, 73-80.

Scheffer, M., Carpenter, S., Foley, J.A., Folke, C., Walker, B., 2001. Catastrophic shifts in ecosystems. Nature, 413(6856), 591-596.
Schmidt, A.H., Gonzalez, V.S., Bierman, P.R., Neilson, T.B., Rood, D.H., 2018. Agricultural land use doubled sediment loads in western China's rivers. Anthropocene, 21, 95-106.
Schneider, L., Lejot, J., Mialhe, F., Landon, N., Jacob-Rousseau, N., Rouet, I., Navratil, O., 2018. The Thio River'S delta: A biogeomorphological recorder of the mining activities in New-Caledonia since 1870.
Schwertmann, U., Latham, M., 1986. Properties of iron oxides in some New Caledonian oxisols. Geoderma, 39, 105-123.
Sellier, V., Navratil, O., Laceby, J.P., Allenbach, M., Lefèvre, I., Evrard, O., 2020. Investigating the use of fallout and geogenic radionuclides as potential tracing properties to quantify the sources of suspended sediment in a mining catchment in New Caledonia, South Pacific. Journal of Soils and Sediments, 20(2), 1112-1128.
Sevin, B., 2014. Cartographie du régolithe sur formation ultrabasique de Nouvelle-Calédonie: Localisation dans l'espace et le temps des gisements nickélifères, Nouvelle Calédonie.
Shellberg, J., Brooks, A., Spencer, J., 2010. Land-use change from indigenous management to cattle grazing initiates the gullying of alluvial soils in northern Australia, 19th World Congress of Soil Science: Soil Solutions for a Changing World, pp. 1-6.
Smith, H.G., Sheridan, G.J., Lane, P.N.J., Noske, P.J., Heijnis, H., 2011. Changes to sediment sources following wildfire in a forested upland catchment, southeastern Australia. Hydrol. Process., 25(18), 2878-2889.
Stinchcomb, G.E., Stewart, R.M., Messner, T.C., Nordt, L.C., Driese, S.G., Allen, P.M., 2013. Using event stratigraphy to map the Anthropocene–An example from the historic coal mining region in eastern Pennsylvania, USA. Anthropocene, 2, 42-50.
Syvitski, J.P., Vörösmarty, C.J., Kettner, A.J., Green, P., 2005. Impact of humans on the flux of terrestrial sediment to the global coastal ocean. science, 308(5720), 376-380.
Terry, J.P., Kostaschuk, R.A., Wotling, G., 2008. Features of tropical cyclone-induced flood peaks on Grande Terre, New Caledonia. Water Environ J, 22(3), 177-183.
Trescases, J.J., 1973. Weathering and geochemical behaviour of the elements of ultramafic rocks in New Caledonia. BMRJ. Aust. Geol and Geophys., 141(Canberra), 149-161.
Turney, C.S., Palmer, J., Maslin, M.A., Hogg, A., Fogwill, C.J., Southon, J., Fenwick, P., Helle, G., Wilmshurst, J.M., McGlone, M., 2018. Global peak in atmospheric radiocarbon provides a potential definition for the onset of the anthropocene epoch in 1965. Scientific reports, 8(1), 3293.
Valette-Silver, N.J., 1993. The use of sediment cores to reconstruct historical trends in contamination of estuarine and coastal sediments. Estuaries, 16(3), 577-588.
Walden, J., Slattery, M.C., Burt, T.P., 1997. Use of mineral magnetic measurements to fingerprint suspended sediment sources: approaches and techniques for data analysis. Journal of Hydrology, 202(1-4), 353-372.
Wallbrink, P., Murray, A., Olley, J., Olive, L., 1998. Determining sources and transit times of suspended sediment in the Murrumbidgee River, New South Wales, Australia, using fallout 137Cs and 210Pb. Water Resour Res, 34(4), 879-887.
Zhu, Y.-M., Lu, X., Zhou, Y., 2008. Sediment flux sensitivity to climate change: A case study in the Longchuanjiang catchment of the upper Yangtze River, China. Global and Planetary Change, 60(3-4), 429-442.

Figure captions

Figure 1: Main lithologies (a), location of the rainfall and river monitoring stations (b), location of the sediment core and sediment samples collected along with tributary source classifications (c) conducted in the Thio River catchment, New Caledonia

Figure 2: Sediment core description through visual observations (a), profiles of chromatic indicator a* (b), Ni contents (c), FDVS (d) and grain size fractions (e)

Figure 3: Profile of mining source contributions (between 50-100%) and delineation of sediment core units (*i.e*. test of data homogeneity) within the sediment core

Figure 4: Dating based on the silt size fraction (cyclonic events referenced by n°, Table 4) and estimations of mining source contributions (between 50-100%) within the sediment core

Figure 5: Evolution of Ni ore and mining waste tonnage over the period 1900 – 2017 coupled to chronology of cyclonic events over the period 1952-2017, mining activity intensification and environmental legislation implementation

Table captions

Table 1: Grain size parameters and percentage of grain size fractions (*i.e.* clay, silt, fine, medium and coarse-sized sand) in the sediment sources and the sediment core (<63 µm fraction, mean ± standard deviation)

Table 2: Geochemical element contents (mean ± standard deviation, mean ± SD; minimum, Min; Maximum, Max) in the sediment sources and the sediment core (<63 µm fraction)

Table 3: Results of Mann-Whitney U test and the DFA used to identify the optimum geochemical tracer combination to differentiate sediment sources in the sediment core (<63 µm fraction)

963 **Table 4:** Chronology of cyclonic events over the period 1952-2017. The number of flood refers to the
964 probable flood deposit recorded in the sediment core (top-to-down numbering). Cyclone Alyson (in
965 bold) corresponds to a tipping point in the sediment core

Table 1

Sediment size	Mining tributaries (n= 16)	Non-mining tributaries (n= 8)	Core sections (n= 32)
d10 (µm)	52 ± 38	60 ± 57	17 ± 10
d50 (µm)	210 ± 133	275 ± 201	173 ± 218
d90 (µm)	655 ± 345	742 ± 488	538 ± 248
Clay <2 µm (%)	2 ± 1	3 ± 3	2 ± 1
2 µm < Silt < 63 µm (%)	21 ± 9	30 ± 29	26 ± 9
63 µm < Fine –sized sand <500 µm (%)	55 ± 19	43 ± 19	61 ± 12
500 µm < Medium-sized sand < 1000 µm (%)	12 ± 10	17 ± 14	4 ± 2
1000 µm < Coarse-sized sand <2000 µm (%)	10 ± 20	7 ± 9	6 ± 14

Table 2

	Mining tributaries (n= 16)		Non-mining tributaries (n= 8)		Core sections (n= 32)	
	Mean ± SD	Min-Max	Mean ± SD	Min-Max	Mean ± SD	Min-Max
Geochemical elements						
Al *(g kg^{-1})*	21 ± 21	4 – 71	67 ± 8	51 – 78	38 ± 10	19 – 53
Ca *(g kg^{-1})*	3.7 ± 0.5	0.3 – 15.0	9.3 ± 5.2	4.5 – 21.1	3.0 ± 2.8	1.1 – 4.4
Cr *(g kg^{-1})*	7.5 ± 4.6	1.8 – 17.7	0.7 ± 1.0	0.05 – 2.9	6.1 ± 1.4	4.0 – 9.0
Fe*(g kg^{-1})*	144 ± 70	63 – 256	62 ± 24	48 – 119	187 ± 43	120 -288
K *(g kg^{-1})*	1.6 ± 2.2	0.1 – 7.0	14.0 ± 3.7	5.8 – 17.4	4.6 ± 1.8	1.2 – 7.3
Mg *(g kg^{-1})*	99 ± 59	16 – 202	16 ±13	5 – 37	67 ± 7	53 – 81
Mn *(g kg^{-1})*	2.5 ± 1.3	1.2 – 4.8	1.4 ± 0.6	1.0 – 2.5	2.9 ± 0.5	1.9 – 3.8
Ni *(g kg^{-1})*	6.6 ± 5.1	0.6 – 17.2	0.3 ± 0.3	0.1 – 0.9	7.6 ± 3.3	2.9 – 15.5
Si *(g kg^{-1})*	178 ± 42	52 – 230	254 ± 28	196 – 281	193 ± 22	154 – 227
Ti *(mg kg^{-1})*	1.4 ± 2.1	0.02 – 5.9	5.4 ± 0.8	4.5 – 7.0	2.6 ± 0.9	0.9 – 4.1
Zn *(mg kg^{-1})*	146 ± 47	91 – 224	125 ± 4	118 – 130	172 ± 31	129 – 262

Table 3

	Mann-Whitney U test		DFA- backward mode			
Fingerprinting property	U value	p value	Wilk's Lambda	Variance explained by the variables (%)	Squared Mahalanobis distance	Correctly classified samples (%)
Al	8	0.000	-	-	-	-
Ca	21	0.007	-	-	-	-
Cr	124	< 0.0001	-	-	-	-
K	2	< 0.0001	0.1691	83.1	20.3	96
Mg	119	0.000	-	-	-	-
Mn	108	0.006	-	-	-	-
Ni	125	< 0.0001	-	-	-	-
Si	6	< 0.0001	-	-	-	-
Ti	13	0.001	-	-	-	-
Zn	**68**	**0.834**	**-**	**-**	**-**	**-**

Table 4

N°	Year	Month, day	Type of event/name	Peak daily ($m^3 s^{-1}$)	*Davar* discharge database	Rainfall-runoff analysis	*Météo France* database	Local testimonies
not recorded in the sediment core	*2017*	*April, 10*	*Cyclone, Cook*	*796*	•		•	•
1	2015	February, 25	Cyclone, Marcia	860	•		•	•
2	2013	July, 1	No-name	na				•
3	2013	February, 1	Cyclone, Freda	1182	•		•	•
4	2009	March, 25	Tropical depression, Jasper	829	•		•	•
5	2008	March, 22	No-name	931	•			
6	2008	February, 28	No-name	825	•			•
7	1996	March, 27	Cyclone, Beti	2014	•		•	•
8	1990	January, 23	No-name	900	•			•
9	1988	January, 12	Cyclone, Anne	na		•	•	•
10	**1975**	**March, 7**	**Cyclone, Alison**	**na**		•	•	•
11	1967	March, 23	No-name	na		•		
12	1959	January, 16	Cyclone, Béatrice	na		•	•	
13	1957	January, 6	No-name	na				

Figure 1

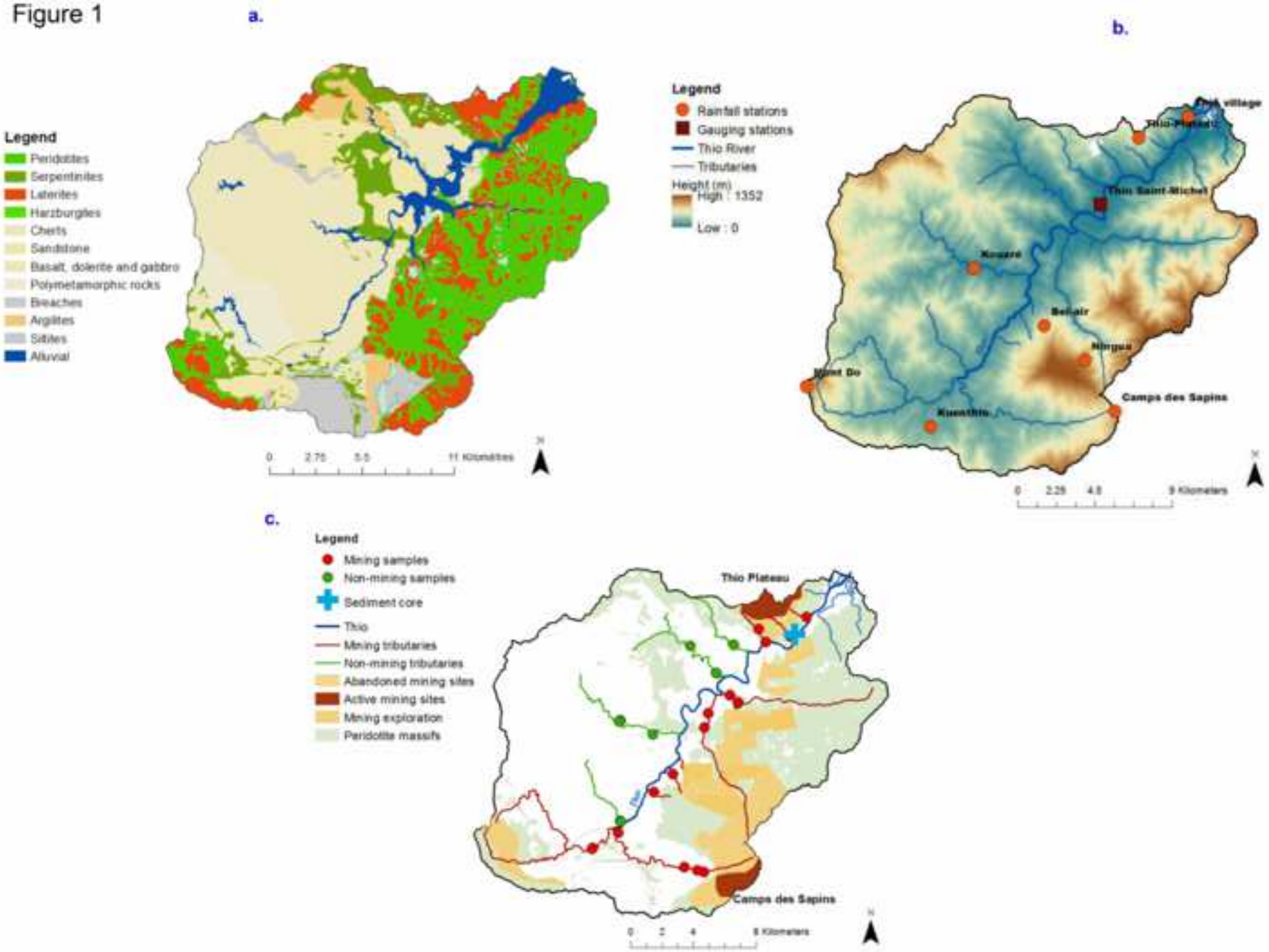
Figure 1
a.
Legend
Peridotites
Serpentinites
Laterites
Harzburgites
Cherts
Sandstone
Basalt, dolerite and gabbro
Polymetamorphic rocks
Breaches
Argilites
Siltites
Alluvial
0 2.75 5.5 11 Kilometres
N
b.
Legend
Rainfall stations
Gauging stations
Thio River
Tributaries
Height (m)
High : 1352
Low : 0
Thio Saint-Michel
Kouaré
Belair
Nimgua
Mont Do
Kuenthio
Camps des Sapins
0 2.25 4.5 9 Kilometers
N
c.
Legend
Mining samples
Non-mining samples
Sediment core
Thio
Mining tributaries
Non-mining tributaries
Abandoned mining sites
Active mining sites
Mining exploration
Peridotite massifs
Thio Plateau
Camps des Sapins
0 2 4 8 Kilometers
N

Figure 2

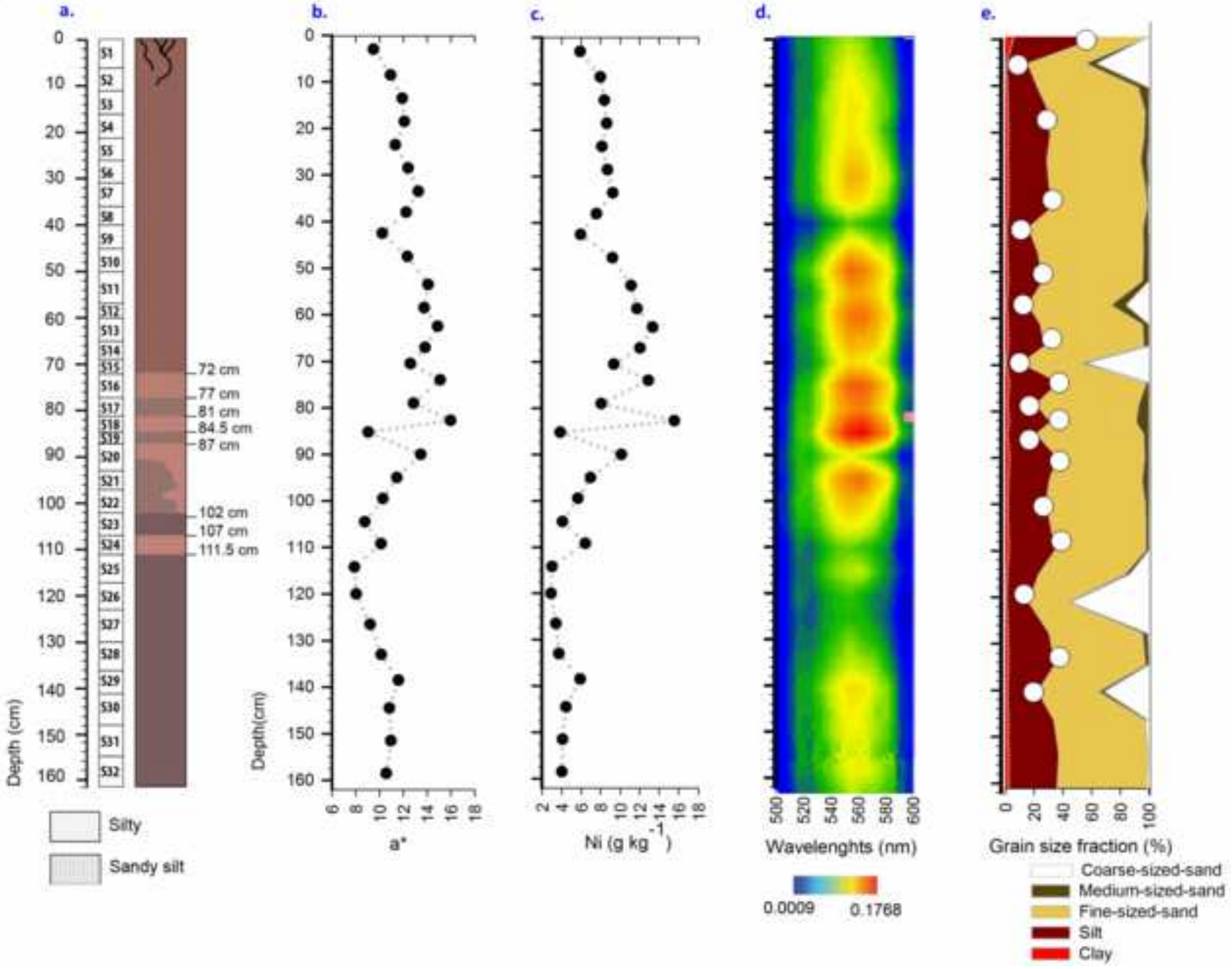
Figure 2
a.
b.
c.
d.
e.
Depth (cm)
72 cm
77 cm
81 cm
84.5 cm
87 cm
102 cm
107 cm
111.5 cm
Silty
Sandy silt
Depth(cm)
a*
Ni (g kg-1)
Wavelenghts (nm)
0.0009
0.1768
Grain size fraction (%)
Coarse-sized-sand
Medium-sized-sand
Fine-sized-sand
Silt
Clay

Figure 3

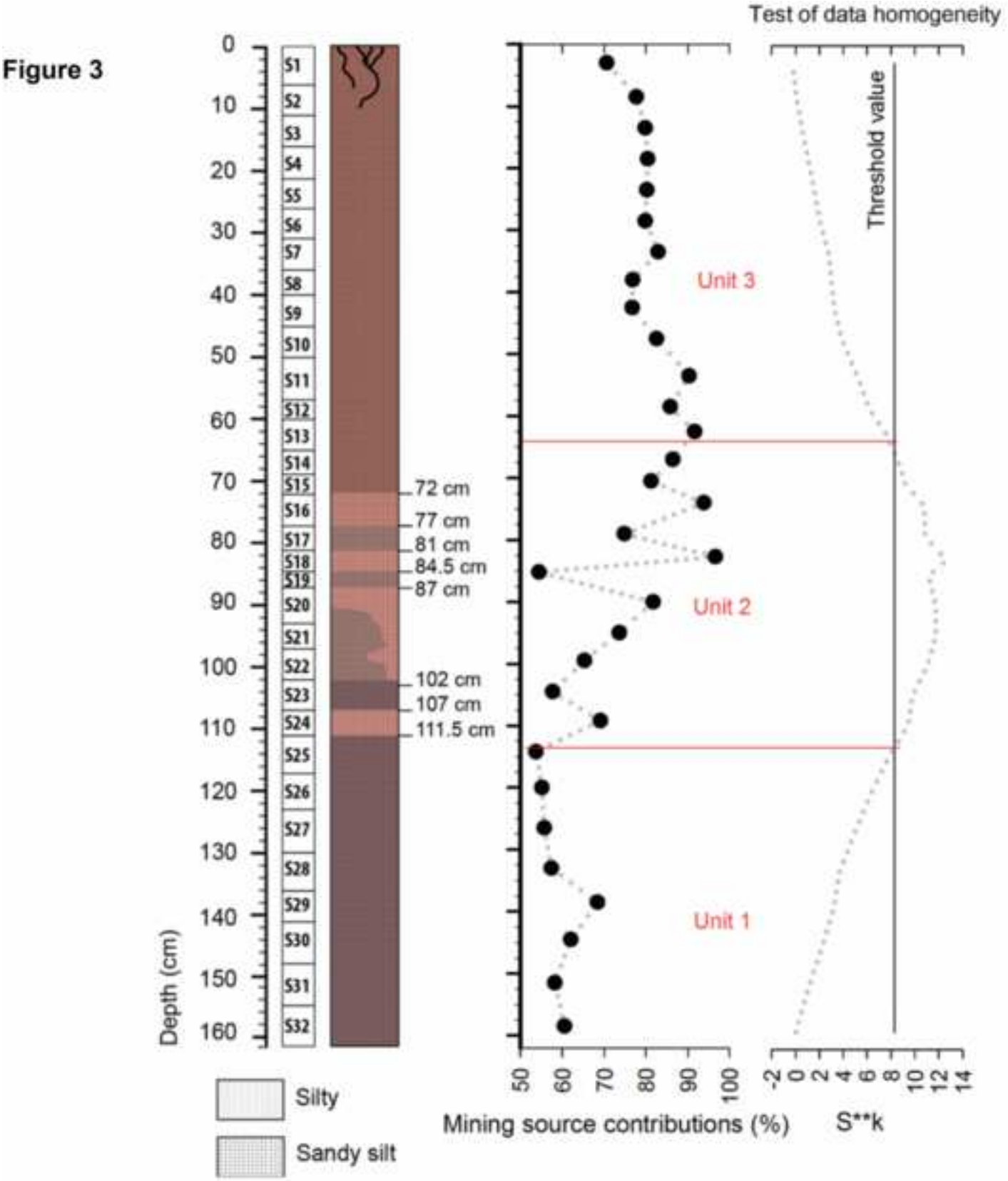
Test of data homogeneity
Threshold value
Unit 3
Unit 2
Unit 1
72 cm
77 cm
81 cm
84.5 cm
87 cm
102 cm
107 cm
111.5 cm
Depth (cm)
Silty
Sandy silt
Mining source contributions (%)
S**k

Figure 4

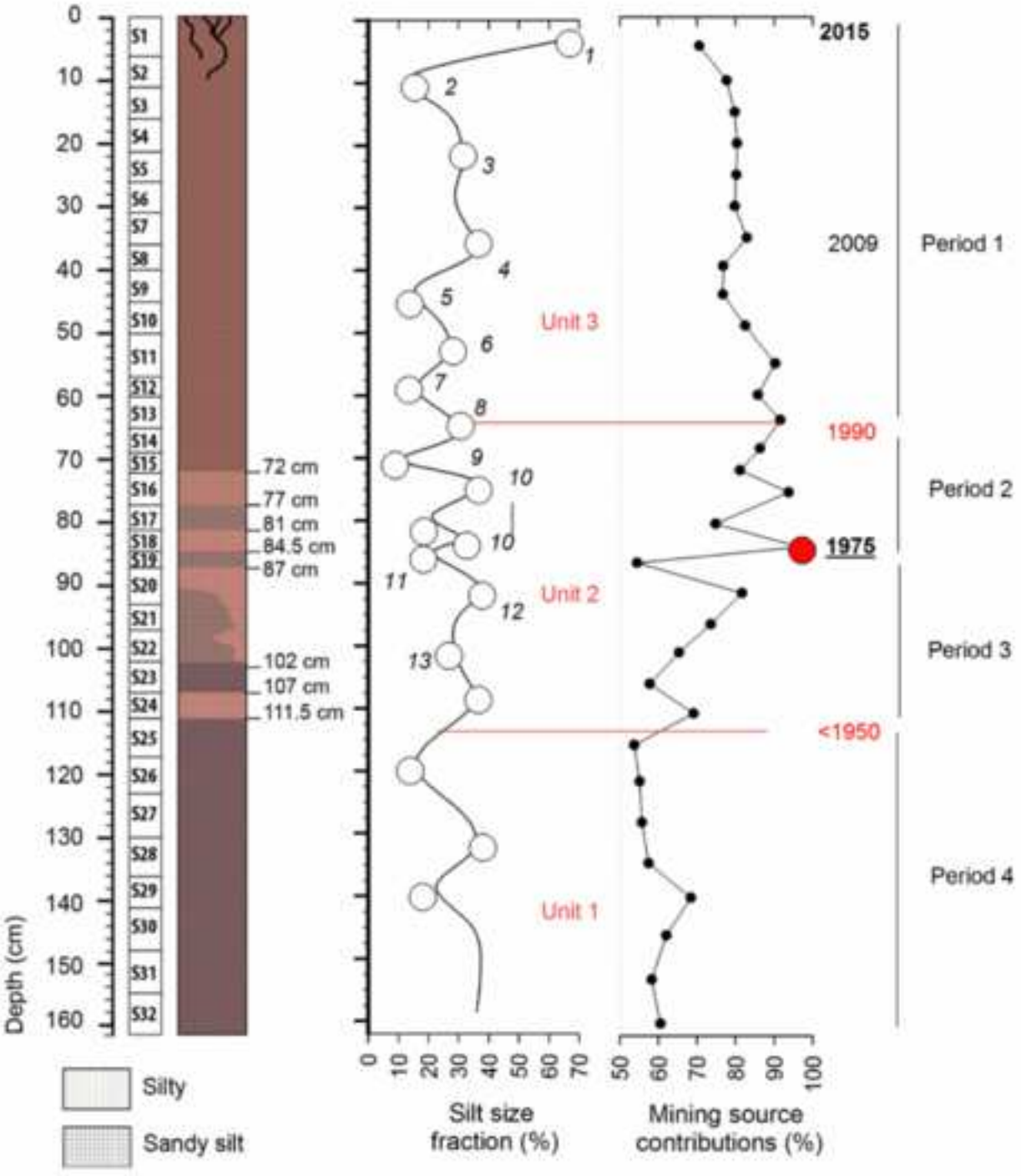
Figure 4
Depth (cm)
0
10
20
30
40
50
60
70
80
90
100
110
120
130
140
150
160
S1
S2
S3
S4
S5
S6
S7
S8
S9
S10
S11
S12
S13
S14
S15
S16
S17
S18
S19
S20
S21
S22
S23
S24
S25
S26
S27
S28
S29
S30
S31
S32
72 cm
77 cm
81 cm
84.5 cm
87 cm
102 cm
107 cm
111.5 cm
Silty
Sandy silt
1
2
3
4
5
6
7
8
9
10
10
11
12
13
Unit 3
Unit 2
Unit 1
0
10
20
30
40
50
60
70
Silt size fraction (%)
2015
2009
1990
1975
<1950
50
60
70
80
90
100
Mining source contributions (%)
Period 1
Period 2
Period 3
Period 4

Figure 5

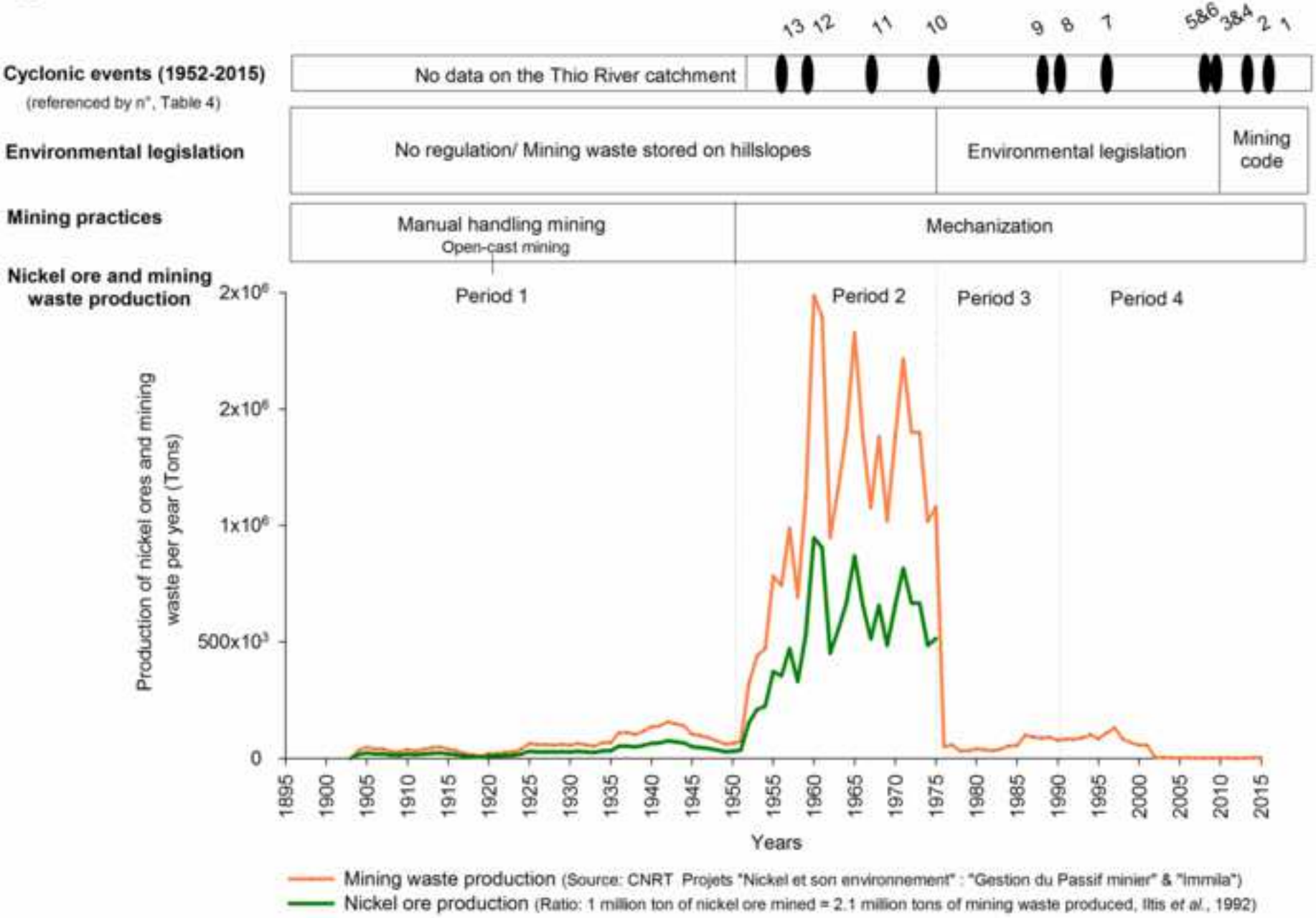
Figure 5
Cyclonic events (1952-2015)
(referenced by n°, Table 4)
13 12 11 10 9 8 7 5&6 3&4 2 1
No data on the Thio River catchment
Environmental legislation
No regulation/ Mining waste stored on hillslopes
Environmental legislation
Mining code
Mining practices
Manual handling mining
Open-cast mining
Mechanization
Nickel ore and mining waste production
Period 1
Period 2
Period 3
Period 4
Production of nickel ores and mining waste per year (Tons)
2x10⁶
2x10⁶
1x10⁶
500x10³
0
1895 1900 1905 1910 1915 1920 1925 1930 1935 1940 1945 1950 1955 1960 1965 1970 1975 1980 1985 1990 1995 2000 2005 2010 2015
Years
Mining waste production (Source: CNRT Projets "Nickel et son environnement" : "Gestion du Passif minier" & "Immila")
Nickel ore production (Ratio: 1 million ton of nickel ore mined = 2.1 million tons of mining waste produced, Iltis et al., 1992)